Extended Data Figure 1

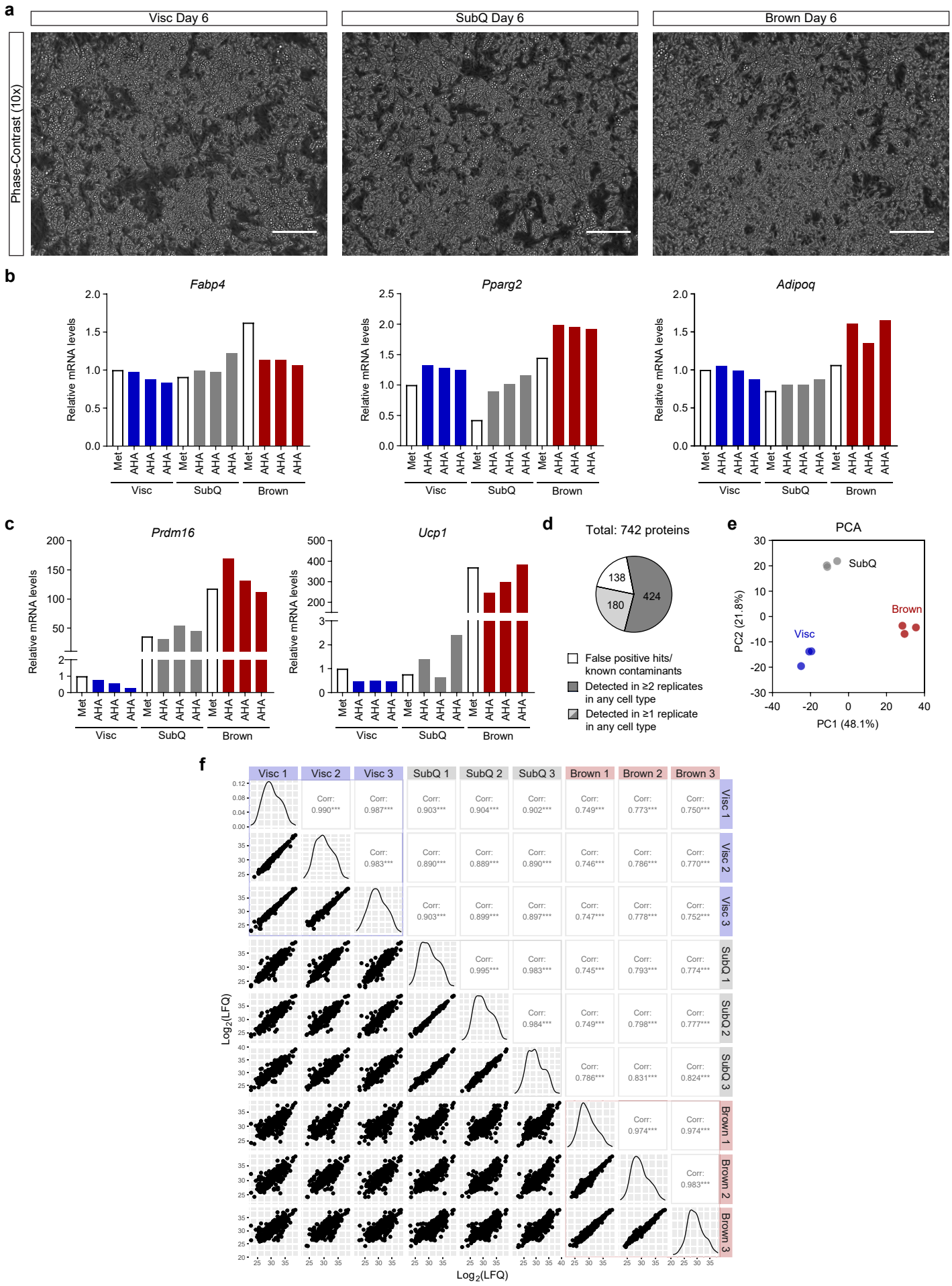

Extended Data Figure 1. Validation of primary adipocyte differentiation and overview of MS results
a, Phase-contrast microscope images of mature Visc, SubQ, and Brown adipocytes on day 6 of differentiation. Scale bars indicate 500 μm.
b, Relative mRNA levels of mature adipocyte genes.
c, Relative mRNA levels of brown fat-enriched genes, *Prdm16* and *Ucp1*.
d, Distribution of detected proteins based on exclusion criteria and number of replicates a protein was detected in.
e, PCA of AHA-pulsed samples.
f, Pairwise comparisons of AHA-pulsed samples. Scatterplot Log_2(LFQ) intensities are displayed on the bottom-left, distribution on the diagonal, and Pearson correlation coefficients on the top-right.

Extended Data Figure 2

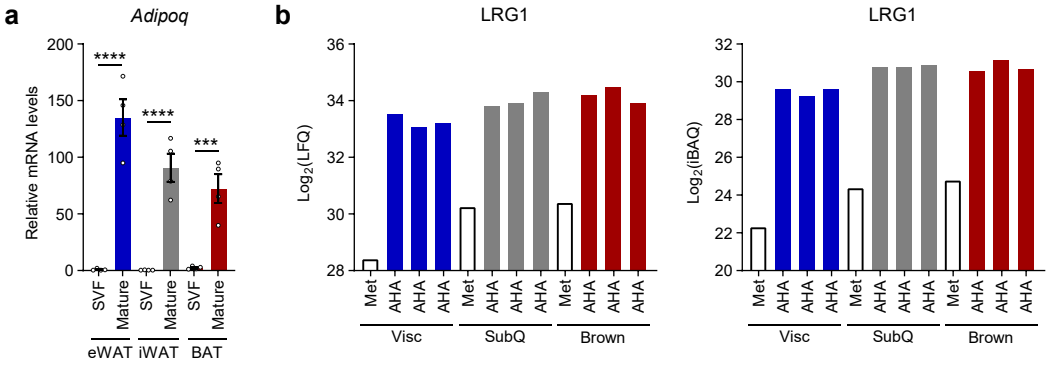

Extended Data Figure 2. Validation of tissue fractionation and MS quantification of LRG1 in adipocyte CM
a, Relative *Adipoq* mRNA levels of indicated tissues fractionated into mature adipocytes and SVF. Data are presented as mean ± SEM. ***P < 0.001, ****P < 0.0001 vs. SVF, from Šídák post hoc test following two-way ANOVA. n = 4 per group.
b, LRG1 Log_2(LFQ) and Log_2(iBAQ) intensities detected by MS analysis of alkyne-agarose enriched CM.

Extended Data Figure 3

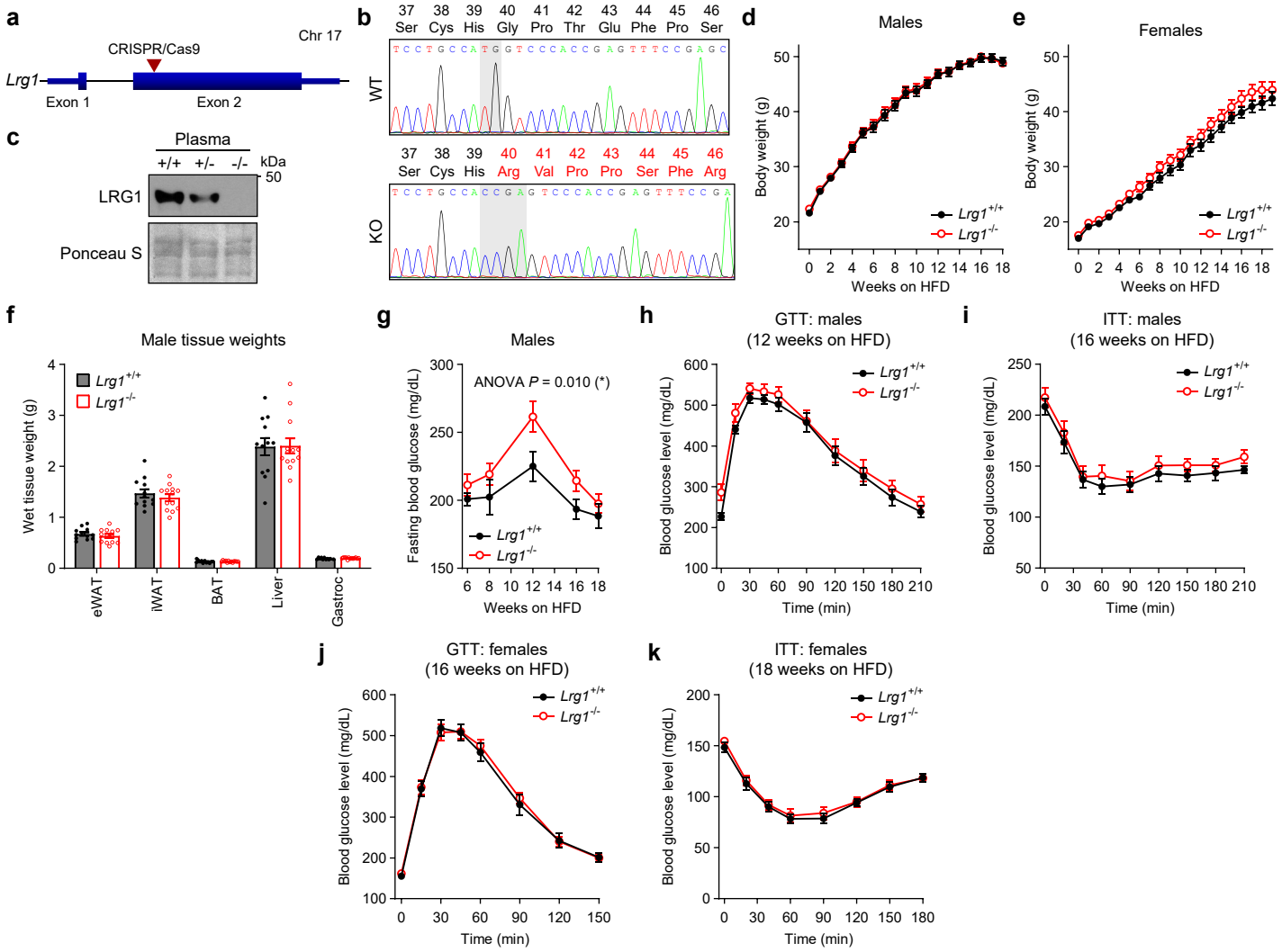

Extended Data Figure 3. LRG1 loss of function in C57BL/6J DIO mice elevates fasting blood glucose

a, Schematic diagram of murine *Lrg1* exon structure. Red arrowhead indicates the region targeted by CRISPR/Cas9 gRNA.

b, Sanger sequencing chromatogram of PCR products amplifying a portion of *Lrg1* exon 2. Shaded portion highlights where sequences differ between WT and LRG1-KO alleles. LRG1 amino acid positions and residues encoded by each allele are indicated above each trace.

c, Western blot of LRG1 in plasma of WT (+/+), LRG1-heterozygote (+/-), and LRG1-KO (-/-) mice.

d, Body weights of LRG1-KO and WT littermate males on HFD started at 6 weeks of age.

e, Body weights of LRG1-KO and WT littermate females on HFD started at 6 weeks of age.

f, Dissected tissue weights from LRG1-KO and WT littermate males at 24 weeks of age (18 weeks on HFD).

g, 6 h fasting blood glucose levels of LRG1-KO and WT littermate males during HFD feeding. ANOVA *P* indicates group factor *P*-values from repeated measures two-way ANOVA. **P* < 0.05.

h, Intraperitoneal glucose tolerance test (1.5 g/kg) in LRG1-KO and WT littermate male mice performed at 18 weeks of age (12 weeks on HFD).

i, Insulin tolerance test (1.5 U/kg) in LRG1-KO and WT littermate male mice performed at 22 weeks of age (16 weeks on HFD).

j, Intraperitoneal glucose tolerance test (1.75 g/kg) in LRG1-KO and WT littermate female mice performed at 22 weeks of age (16 weeks on HFD).

k, Insulin tolerance test (1.0 U/kg) in LRG1-KO and WT littermate female mice performed at 24 weeks of age (18 weeks on HFD).

Data are presented as mean ± SEM. Males: *n* = 12 for WT and *n* = 13 for LRG1-KO. Females: *n* = 12 for WT and *n* = 16 for LRG1-KO.

Extended Data Figure 4

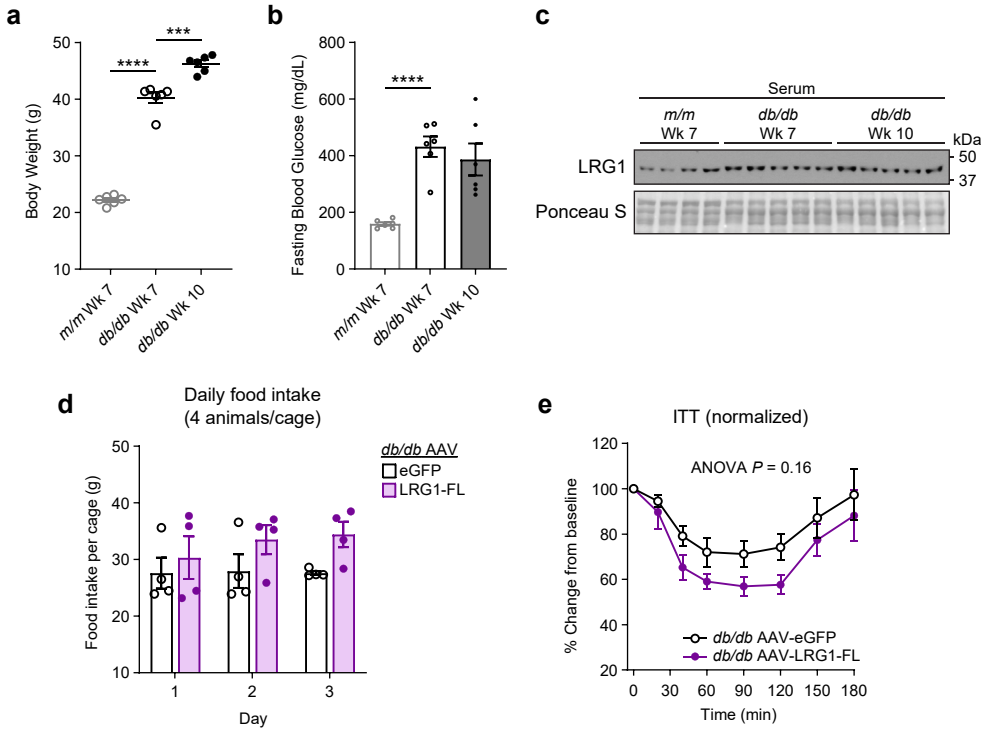

Extended Data Figure 4. Metabolic characterization of *db/db* vs. *m/m* mice and AAV-transduced *db/db* mice

a, Body weights of *db/db* and littermate *m/m* male mice at 7 and 10 weeks of age. ***$P < 0.001$, ****$P < 0.0001$ from two-sided Welch's *t*-test. $n = 6$ per group.

b, 6 h fasting blood glucose levels of *db/db* and littermate *m/m* male mice at 7 and 10 weeks of age. ****$P < 0.0001$ from two-sided Welch's *t*-test. $n = 6$ per group.

c, Western blot of LRG1 in serum of *db/db* and littermate *m/m* male mice.

d, Daily food intake per cage housing 4 AAV-transduced *db/db* male mice. $n = 4$ per group.

e, Normalized insulin tolerance test data from Fig. 5f. ANOVA *P* indicates group factor *P*-value from repeated measures two-way ANOVA.

Data are presented as mean ± SEM.

Extended Data Figure 5

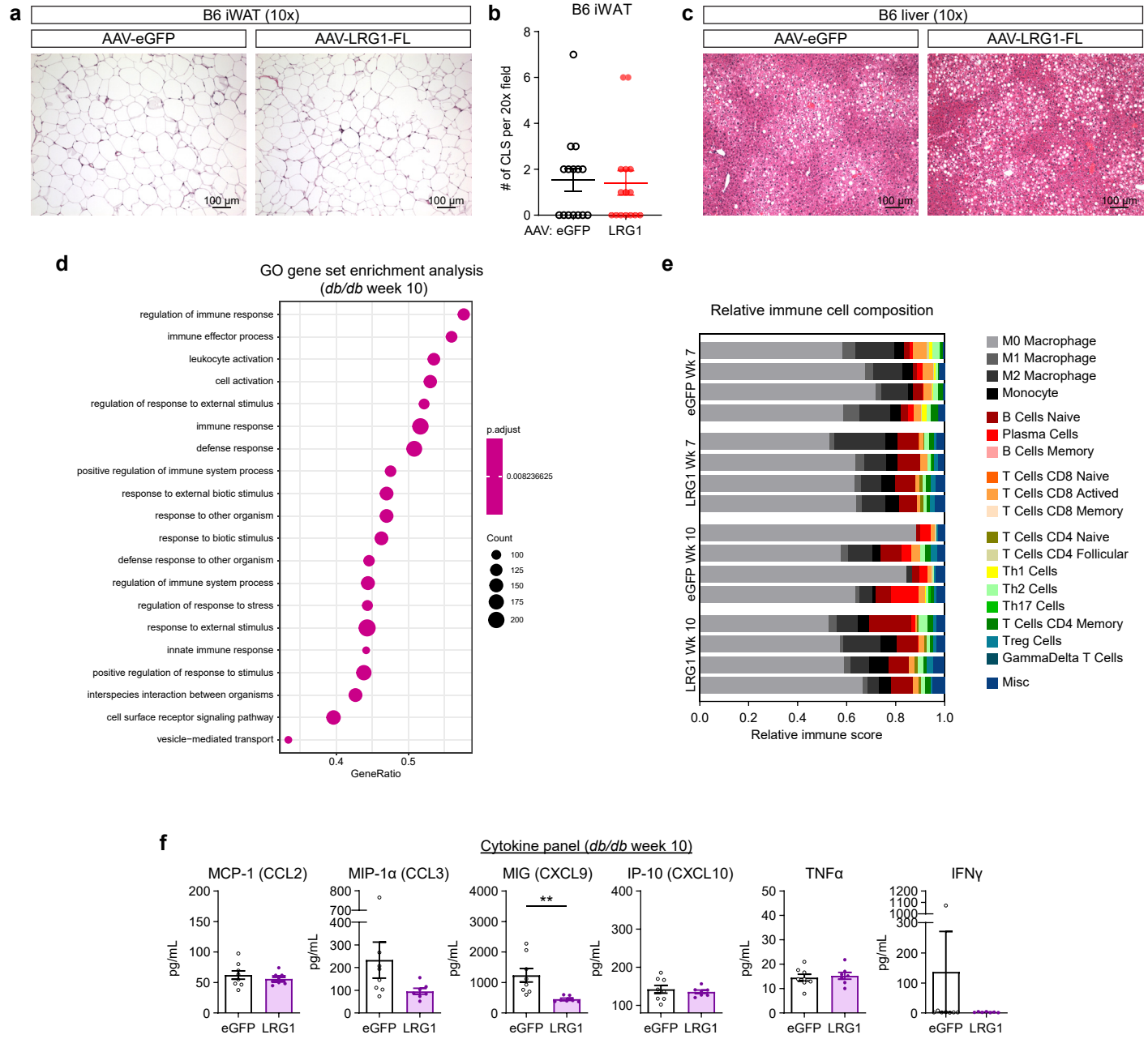

Extended Data Figure 5. Analysis of inflammatory phenotypes with LRG1 gain of function

a, Representative images from H&E-stained iWAT sections from B6 DIO mice transduced with AAV-eGFP or AAV-LRG1-FL. Scale bars are indicated.

b, Quantification of CLS from **a**. Data are presented as mean ± SEM.

c, Representative images from H&E-stained liver sections from B6 DIO mice transduced with AAV-eGFP or AAV-LRG1-FL. Scale bars are indicated.

d, Top 20 enriched GO BP pathways from GSEA of significantly differentially expressed genes in eWAT between *db/db*-LRG1 and *db/db*-eGFP at 10 weeks of age.

e, Relative scores from immune cell type deconvolution analysis of eWAT transcriptomes using CIBERSORTx.

f, Quantification of serum chemokine/cytokine levels in *db/db*-LRG1 and *db/db*-eGFP at 10 weeks of age. Data are presented as mean ± SEM. $^{**}P < 0.01$ from two-sided Welch's *t*-test. $n = 8$ for *db/db*-eGFP and $n = 7$ for *db/db*-LRG1.

Extended Data Figure 6

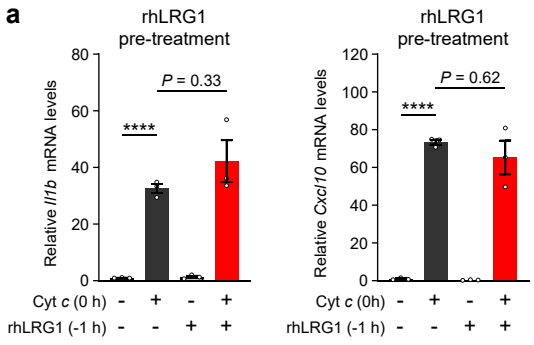

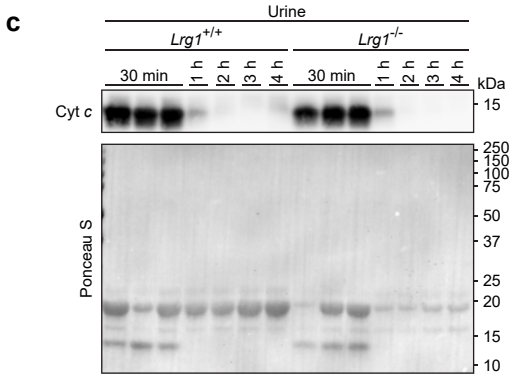

b

$Y = Plateau + (Y0 - Plateau)e^{-K*X}$

	WT (*Lrg1*$^{+/+}$)	KO (*Lrg1*$^{-/-}$)
Best-fit values		
Y0	1.173	1.297
Plateau	0.2791	-0.0007925
K	0.04306	0.04002
Half Life	16.10	17.32
Tau (1/K)	23.23	24.99
Span	0.8936	1.298
95% CI (profile likelihood)		
Y0	0.9578 to 1.454	0.9730 to 1.699
Plateau	0.1925 to 0.3608	-0.1380 to 0.1278
K	0.02460 to 0.08768	0.02225 to 0.08035
Half Life	7.905 to 28.18	8.626 to 31.16
Tau (1/K)	11.40 to 40.65	12.44 to 44.95
Goodness of Fit		
Degrees of Freedom	21	21
R squared	0.7971	0.7775
Sum of Squares	0.4115	1.006
Sy.x	0.1400	0.2189

Extended Data Figure 6. Analysis of LRG1-Cyt *c* interaction

a, Relative *Il1b* and *Cxcl10* mRNA levels in BMDMs in response to 20 µg/mL equine Cyt *c* with or without 1 h pre-treatment of 50 µg/mL recombinant human LRG1. Data are presented as mean ± SEM. Tukey post hoc test results from two-way ANOVA are indicated. ****$P < 0.0001$.

b, Table summarizing results from least squares regression fit of relative Cyt *c* intensities with one-phase decay functions.

c, Urine Cyt *c* western blot and Ponceau S stain of urinary proteins from animals in Fig. 7h.